Applied Energy 106 (2013) 79–88

Contents lists available at SciVerse ScienceDirect

Applied Energy

journal homepage: www.elsevier.com/locate/apenergy

Optimal design of thermoelectric devices with dimensional analysis

HoSung Lee *

Mechanical and Aeronautical Engineering, Western Michigan University, 1903 W. Michigan Ave., Kalamazoo, MI 49008-5343, USA

HIGHLIGHTS

- ▶ This paper discusses optimal design of thermoelectric devices with dimensional analysis.
- ▶ A real design example for exhaust gas energy conversion was shown using the dimensional analysis.
- ▶ A real design example for automobile air conditioner was demonstrated using the dimensional analysis.

ARTICLE INFO

Article history:
Received 29 September 2012
Received in revised form 13 January 2013
Accepted 16 January 2013
Available online 14 February 2013

Keywords:
Optimal design
Dimensional analysis
Thermoelectric generator
Thermoelectric cooler
Thermoelectric module

ABSTRACT

The optimum design of thermoelectric devices (thermoelectric generator and cooler) in connection with heat sinks was developed using dimensional analysis. New dimensionless groups were properly defined to represent important parameters of the thermoelectric devices. Particularly, use of the convection conductance of a fluid in the denominators of the dimensionless parameters was critically important, which leads to a new optimum design. This allows us to determine either the optimal number of thermocouples or the optimal thermal conductance (the geometric ratio of footprint of leg to leg length). It is stated from the present dimensional analysis that, if two fluid temperatures on the heat sinks are given, an optimum design always exists and can be found with the feasible mechanical constraints. The optimum design includes the optimum parameters such as efficiency, power, current, geometry or number of thermocouples, and thermal resistances of heat sinks.

1. Introduction

Thermoelectric devices (thermoelectric generator and cooler) have found comprehensive applications in solar energy conversion [1], exhaust energy conversion [2,3], low grade waste heat recovery [4–6], power plants [7], electronic cooling [8], vehicle air conditioners, and refrigerators [7]. The most common refrigerant used in home and automobile air conditioners is R-134a, which does not have the ozone-depleting properties of Freon, but is nevertheless a terrible greenhouse gas and will be banned in the near future [9]. The pertinent candidate for the replacement would be thermoelectric coolers. Many analyses, optimizations, even manufacturers' performance curves on thermoelectric devices have been based on the constant high and cold junction temperatures of the devices. Practically, the thermoelectric devices must work with heat sinks (or heat exchangers). It is then very difficult to have the constant junction temperatures unless the thermal resistances of the heat sinks are zero, which is, of course, impossible.

A significant amount of research related to the optimization of thermoelectric devices in conjunction with heat sinks has been conducted as found in the literature [10–30]. It is well noted from the literature that there is the existence of optimal conditions in power output or efficiency with respect to the external load resistance for a thermoelectric generator (TEG) or the electrical current for a thermoelectric cooler (TEC). Many researchers attempted to combine the theoretical thermoelectric equations and the heat balance equations of heat sinks, and then to optimize design parameters such as the geometry of heat sinks [10], allocation of the heat transfer areas of heat sinks [12,13,18,19], thermoelement length [14], the number of thermocouples [15], the geometric ratio of the cross-sectional area of thermoelement to the length [16], and slenderness ratio (the geometric factor ratio of n-type to that of p-type elements) [17]. It can be seen from the above literature that the geometric optimization of thermoelectric devices is important in design and also formidable due to so many design parameters. The thermal conductance of thermoelements that is the most important geometric parameter has been often addressed in analysis, which is the product of three parameters: the number of thermocouples, the geometric ratio, and the thermal conductivity. In order to reduce the optimum design parameters, obviously dimensionless analyses were performed in the literature [21–26]. Yamanashi [21] developed optimum design introducing dimensionless parameters for a thermoelectric cooler with two heat

* Tel.: +1 269 276 3429 (O); fax: +1 269 276 3421.
E-mail address: hosung.lee@wmich.edu

0306-2619/$ - see front matter © 2013 Elsevier Ltd. All rights reserved.
http://dx.doi.org/10.1016/j.apenergy.2013.01.052

Nomenclature

A	cross-sectional area of thermoelement (cm^2)
A_1	total fin surface area at fluid 1 (cm^2)
A_2	total fin surface area at fluid 2 (cm^2)
A_b	base area of heat sink (cm^2)
COP	the coefficient of performance
h_1	heat transfer coefficient of fluid 1 (W/m^2 K)
h_2	heat transfer coefficient of fluid 2 (W/m^2 K)
I	electric current (A)
L	length of thermoelement (mm)
k	thermal conductivity (W/m K), $k = k_p + k_n$
n	the number of thermocouples
N_k	dimensionless thermal conductance $N_k = n(Ak/L)/\eta_2 h_2 A_2$
N_h	dimensionless convection, $N_h = \eta_1 h_1 A_1/\eta_2 h_2 A_2$
N_I	dimensionless current, $N_I = \alpha I/(Ak/L)$
N_V	dimensionless voltage, $N_V = V_n/(n\alpha T_{\infty 2})$
Q_1	the rate of heat transfer entering into TEG (W)
Q_2	the rate of heat transfer leaving TEG (W)
P_d	power density (W/cm^2)
R	electrical resistance of a thermocouple (Ω)
R_L	load resistance of a thermocouple (Ω)
R_r	dimensionless resistance, $R_r = R_L/R$
T_1	junction temperature at fluid 1 (°C)
T_2	junction temperature at fluid 2 (°C)
$T_{\infty 1}$	temperature of fluid 1 (°C)
$T_{\infty 2}$	temperature of fluid 2 (°C)
$T_{\infty 1,\max}$	maximum temperature of fluid 1 (°C)
$T_{\infty 1,\min}$	minimum temperature of fluid 1 (°C)
V_n	voltage of a module (V)
W_n	power output (W)
W_n	power input (W)
Z	the figure of merit

Greek symbols

α	Seebeck coefficient (V/K), $\alpha = \alpha_p - \alpha_n$
ρ	electrical resistivity (Ω cm), $\rho = \rho_p + \rho_n$
η_1	fin efficiency of heat sink 1
η_2	fin efficiency of heat sink 2
η_{th}	thermal efficiency of TEG

Subscripts

p	p-type element
n	n-type element
opt	optimal quantity
$1/2opt$	half optimal quantity

Superscript

$*$	dimensionless

sinks, wherein the thermal conductance appears twice in the nominators and fourth in the denominators of the dimensionless parameters. Although his work led to a new approach in dimensionless optimum design, the analysis encountered difficulties in optimizing the cooling power with respect to the thermal conductance because the conductance is intricately related to the others. Later, researchers [22,24,25] reported optimum design using the similar dimensionless parameters used by Yamanashi [21], presenting valuable optimum design features as Xuan [22] optimized cooling power for a TEC as a function of thermoelement length, Pan et al. [24] showed the optimum thermal conductance for a TEC with a given cooling power, and Casano and Piva [25] presented the optimum external load resistance ratio with heat sinks for a TEG which is greater than unity. There are also some experimental works [27–30] comparing with the theoretical thermoelectric equations. Gou et al. [27] conducted experiments for low-temperature waste heat recovery and demonstrated that the experimental results were in fair agreement with the solution formulas originally derived by Chen et al. [15] from the general theoretical thermoelectric equations. Chang et al. [28] and Huang et al. [29] conducted experiments for a TEC from a heat source with air-cooling and water cooling heat sinks, respectively. Casano and Piva [30] reported experimental work on a set of nine thermoelectric generator modules with a heat source on one side and a heat sink on the other side. After deliberately determined the heat leakage which turned out to be about 30% of the supplied heat source, they demonstrated that the theoretical performance curves of the power output and efficiency as a function of the external load resistance and temperature difference were in good agreement with the measurements. It is realized from the above experimental works that the theoretical thermoelectric equations with the heat balance equations of heat sinks can reasonably predict the real performance. However, proper optimum design still remains questionable.

In spite of many efforts for optimum design, its applications seem greatly challenging to system designers [1–3]. For example, Hsu et al. [3] in 2011 tested an exhaust heat recovery system both experimentally using an automobile and mathematically using computer simulations. They found a reasonable agreement between the measurements and the simulations. However, they obtained the power output of 12.41 W over 24 thermoelectric generator modules with the exhaust gas temperature of 573 K and the air temperature of 300 K. When the power output was divided by the footprint of 24 thermoelectric generator modules, it gives the power density of 0.032 W/cm^2, which seems unusually small. Karri et al. [2] in 2012 conducted a similar experiment with an SUV automobile. This time they designed the exhaust heat recovery system with an optimum coolant flow rate. They obtained the power output of 550 W over 16 thermoelectric generator modules with the exhaust gas temperature of 686 K and the coolant temperature of 361 K, which provided the power density of 0.61 W/cm^2. This shows a significant improvement, indicating the importance of optimum design. A New Energy Development Organization (NEDO) Program (Japan) [7] in 2003 also reported a similar experiment with a passenger car, obtaining the power output of 240 W over 16 segmented-type modules with the exhaust gas temperature of 773 K and the coolant temperature of 298 K, which provided the power density of $\sim$1 W/cm^2. Notably, the power densities obtained are no way to evaluate how good it is until the better comes because proper optimum design seems not available.

From the review of the above theoretical and experimental studies including optimum design in the literature, it is summarized that the proper optimum design should be determined basically not only by the power output for TEG (or cooling power for TEC) but also by the efficiency (the coefficient of performance) simultaneously with respect to both the external load resistance (or the electrical current) and the geometry of thermoelement which refers to the number of thermocouples and the geometric ratio. The former (external load resistance) is well attained in the literature but the latter (geometry) is vague. Therefore, the optimum design seems incomplete. This is the rationale why the present paper is to improve the optimum design introducing new dimensionless parameters.

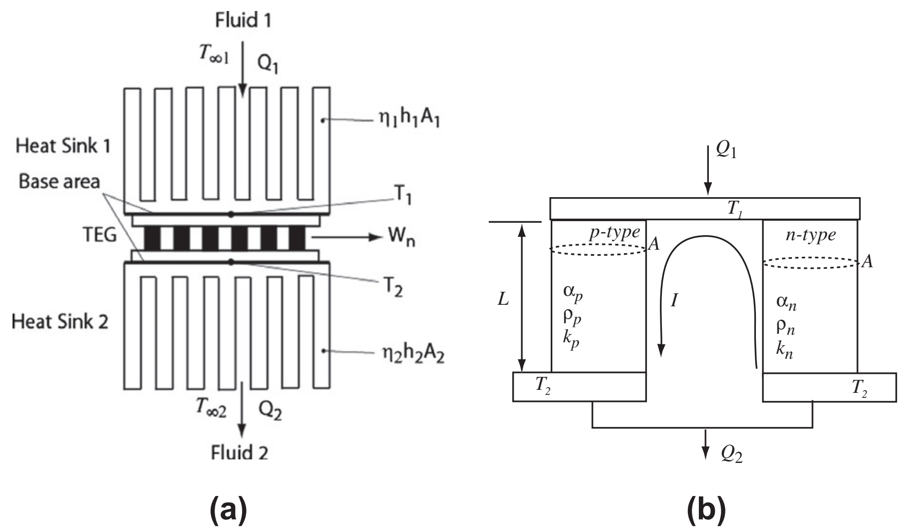

Fig. 1. (a) Thermoelectric generator module (TEG) with two heat sinks and (b) thermocouple.

1.1. Thermoelectric generator

Let us consider a simplified steady-state heat transfer on a thermoelectric generator module (TEG) with two heat sinks as shown in Fig. 1a. Each heat sink faces a fluid flow at temperature T_∞. Subscripts 1 and 2 denote hot and cold quantities, respectively. We assume that the electrical and thermal contact resistances in the TEG are negligible, the material properties are independent of temperature, and also the TEG is perfectly insulated. The TEG has a number of thermocouples, of which each thermocouple consists of p-type and n-type thermoelements with the same dimensions as shown in Fig. 1b. It is noted that the thermal resistance of heat sink 1 can be expressed by the reciprocal of the convection conductance $\eta_1 h_1 A_1$, where η_1 is the fin efficiency, h_1 is the convection coefficient, and A_1 is the total surface area in the heat sink 1. We hereafter use the convection conductance rather than the thermal resistance. The basic equations for the TEG with two heat sinks are given by

$$Q_1 = \eta_1 h_1 A_1 (T_{\infty 1} - T_1) \tag{1}$$

$$Q_1 = n\left(\alpha I T_1 - \frac{1}{2} I^2 R + \frac{Ak}{L}(T_1 - T_2)\right) \tag{2}$$

$$Q_2 = n\left(\alpha I T_2 + \frac{1}{2} I^2 R + \frac{Ak}{L}(T_1 - T_2)\right) \tag{3}$$

$$Q_2 = \eta_2 h_2 A_2 (T_2 - T_{\infty 2}) \tag{4}$$

$$I = \frac{\alpha (T_1 - T_2)}{R_L + R} \tag{5}$$

where $\alpha = \alpha_p - \alpha_n$, $k = k_p + k_n$, and $\rho = \rho_p + \rho_n$. Eqs. (1)–(5) can be solved for T_1 and T_2, providing the power output. However, in order to study the optimization of the TEG, several dimensionless parameters are introduced. As mentioned in Section of Introduction, it is reminded that optimum design should consider not only the power output but also the efficiency simultaneously with respect to both the external load resistance and the geometry of thermoelement which refers to the number of thermocouples and the geometric ratio. In order to reveal the effect of thermal conductance $n(Ak/L)$, the thermal conductance is placed in the nominator while the convection conductance $\eta_2 h_2 A_2$ in fluid 2 is placed in the denominator of the parameter. The convection conductance $\eta_2 h_2 A_2$ and temperature $T_{\infty 2}$ at fluid 2 are assumed to be given. The dimensionless thermal conductance, the ratio of thermal conductance to the convection conductance in fluid 2, is defined by

$$N_k = \frac{n(Ak/L)}{\eta_2 h_2 A_2} \tag{6}$$

The dimensionless convection is an important geometry of heat sinks. Since the convection conductance at fluid 2 is given as mentioned before, the dimensionless convection, the ratio of convection conductance in fluid 1 to fluid 2, is defined by

$$N_h = \frac{\eta_1 h_1 A_1}{\eta_2 h_2 A_2} \tag{7}$$

The dimensionless electrical resistance, the ratio of the load resistance to the electrical resistance of thermocouple, is given by

$$R_r = \frac{R_L}{R} \tag{8}$$

Since the fluid temperature $T_{\infty 2}$ at fluid 2 is given as mentioned before, the dimensionless temperatures are defined by

$$T_1^* = \frac{T_1}{T_{\infty 2}} \tag{9}$$

$$T_2^* = \frac{T_2}{T_{\infty 2}} \tag{10}$$

$$T_\infty^* = \frac{T_{\infty 1}}{T_{\infty 2}} \tag{11}$$

The dimensionless power and heat transfer are defined by dividing by the product of the convection conductance and the temperature of fluid 2 so that the quantities depend only on the nominators not on the denominators since the denominator is assumed to be constant or given. The two dimensionless rates of heat transfer and the dimensionless power output are defined by

$$Q_1^* = \frac{Q_1}{\eta_2 h_2 A_2 T_{\infty 2}} \tag{12}$$

$$Q_2^* = \frac{Q_2}{\eta_2 h_2 A_2 T_{\infty 2}} \tag{13}$$

$$W_n^* = \frac{W_n}{\eta_2 h_2 A_2 T_{\infty 2}} \tag{14}$$

It is noted that the above dimensionless parameters are based on the convection conductance in fluid 2, which means that $\eta_2 h_2 A_2$ $T_{\infty 2}$ should be initially provided. Also note that the thermal conductance $n(Ak/L)$ appears only in Eq. (6) among other

parameters so that the thermal conductance can be examined for optimization. Using the dimensionless parameters defined in Eqs. (6)–(11), Eqs. (1)–(5) reduce to two formulas as:

$$\frac{N_h(T_\infty^* - T_1^*)}{N_k} = \frac{ZT_{\infty 2}(T_1^* - T_2^*)T_1^*}{R_r + 1} - \frac{ZT_{\infty 2}(T_1^* - T_2^*)^2}{2(R_r + 1)^2} + (T_1^* - T_2^*) \quad (15)$$

$$\frac{T_2^* - 1}{N_k} = \frac{ZT_{\infty 2}(T_1^* - T_2^*)T_2^*}{R_r + 1} + \frac{ZT_{\infty 2}(T_1^* - T_2^*)^2}{2(R_r + 1)^2} + (T_1^* - T_2^*) \quad (16)$$

where Z is called the figure of merit ($Z = \alpha^2/\rho k$). Eqs. (15) and (16) can be solved for T_1^* and T_2^*. The dimensionless temperatures are then a function of five independent dimensionless parameters as

$$T_1^* = f(N_k, N_h, R_r, T_\infty^*, ZT_{\infty 2}) \quad (17)$$

$$T_2^* = f(N_k, N_h, R_r, T_\infty^*, ZT_{\infty 2}) \quad (18)$$

T_∞^* is the input and $ZT_{\infty 2}$ is the material property with the input, and both are initially provided. Therefore, the optimization can be performed only with the first three parameters (N_k, N_h, and R_r). Once the two dimensionless temperatures (T_1^* and T_2^*) are solved for, the dimensionless rates of heat transfer at both hot and cold junctions of the TEG can be obtained as:

$$Q_1^* = N_h(T_\infty^* - T_1^*) \quad (19)$$

$$Q_2^* = T_2^* - 1 \quad (20)$$

Then, we have the dimensionless power output as

$$W_n^* = Q_1^* - Q_2^* \quad (21)$$

Accordingly, the thermal efficiency is obtained by

$$\eta_{th} = \frac{W_n^*}{Q_1^*} \quad (22)$$

Defining $N_I = \alpha IL/Ak$, the dimensionless current is obtained by

$$N_I = \frac{ZT_{\infty 2}(T_1^* - T_2^*)}{R_r + 1} \quad (23)$$

Also, defining $N_V = V/n\alpha T_{\infty 2}$, the dimensionless voltage is obtained by

$$N_V = \frac{W_n^*}{N_I N_k} \quad (24)$$

With the inputs (T_∞^* and $ZT_{\infty 2}$), we begin developing the optimization with the dimensionless parameters (N_k, N_h, and R_r) iteratively until they converge. It is found that both N_k and R_r show their optimal values for the dimensionless power output, while N_h does not show the optimal value showing that the dimensionless power output monotonically increases with increasing N_h. This implies that, if N_h is given, the optimal combination of N_k and R_r can be obtained. However, the dimensionless convection N_h actually presents the feasible mechanical constraints. Thus, we first proceed with a typical value of $N_h = 1$ for illustration and later examine the variety of N_h with some practical design examples.

Suppose that we have two initial inputs of $T_\infty^* = 2.6$ (two fluid temperatures) and $ZT_{\infty 2} = 1.0$ (materials) along with $N_h = 1$. We then determine the optimal combination for N_k and R_r, which may be obtained either graphically or using a computer program. We first use the graphical method at this moment and later the program for multiple computations. The dimensionless power output W_n^* and thermal efficiency η_{th} are together plotted as a function of R_r, which are presented in Fig. 2a. Both W_n^* and η_{th} with respect to R_r indeed show their optimal values that appear close. We are interested primarily in the power output and secondly in the efficiency. However, since they are close each other, we herein use the power output for the optimization. It should be noted that the dimensionless maximum power output does not occur at $R_r = 1$ from Fig. 2a as usually assumed for a TEG without heat sinks, but approximately at $R_r = 1.7$, because the dimensionless temperatures T_1^* and T_2^* in Fig. 2b are no longer constant. This is often a confusing factor in optimum design with a TEG with two heat sinks. We should not assume that R_r is equal to unity for a TEG with heat sinks.

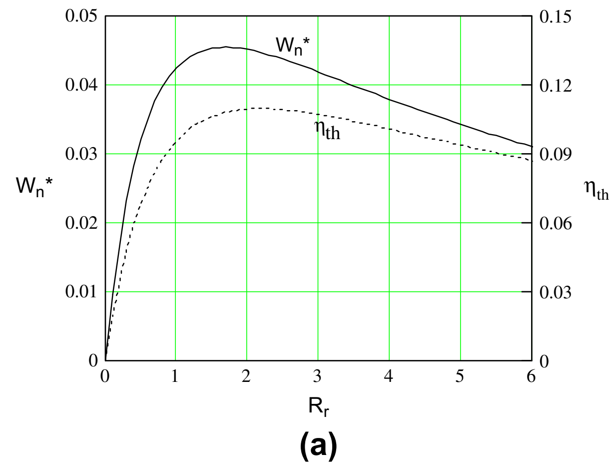

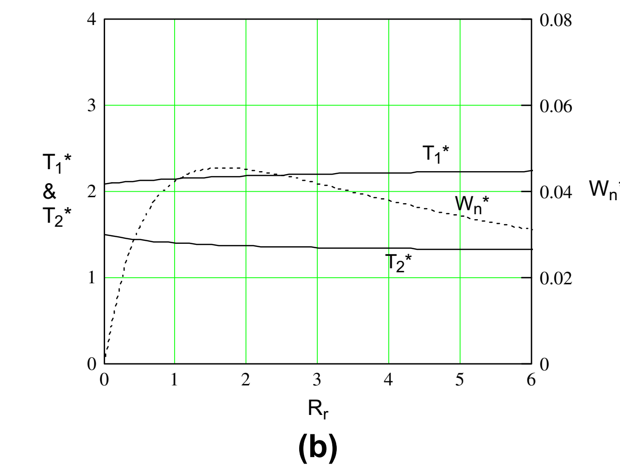

Fig. 2. (a) Dimensionless power output W_n^* and efficiency η_{th} versus the ratio of load resistance to resistance of thermocouple R_r and (b) dimensionless temperatures T_1^* and T_2^* versus R_r. These plots were generated using $N_k = 0.3$, $N_h = 1$, $T_\infty^* = 2.6$ and $ZT_{\infty 2} = 1.0$.

With the dimensionless parameters obtained ($N_h = 1$, $R_r = 1.7$, $T_\infty^* = 2.6$, and $ZT_{\infty 2} = 1.0$), we now plot the dimensionless power output W_n^* as a function of the dimensionless thermal conductance N_k defined in Eq. (6) along with the thermal efficiency η_{th}, which is shown in Fig. 3a. We find an optimum W_n^* approximately at $N_k = 0.3$. Actually, the optimal values of N_k and R_r should be iterated until the two simultaneously converge. From $N_k = n(Ak/L)/\eta_2 h_2 A_2$ as shown in Eq. (6), the N_k actually determines the number of thermocouples n if the geometric ratio A/L and $\eta_2 h_2 A_2$ are given or vice versa. The dimensionless power output W_n^* first increases and later decreases with increasing N_k. It is important to realize that, if $\eta_2 h_2 A_2$ is given, there is an optimal number n of thermocouples (or optimal thermal conductance Ak/L) in the thermoelectric module, which is usually unknown. Physically, the surplus number of thermocouples virtually increases the thermal conduction more than the production of power, which causes the net power output to decline. There is another important aspect of the optimal dimensionless thermal conductance of $N_k = 0.3$, which is that the module thermal conductance nAk/L directly depends on the $\eta_2 h_2 A_2$. In other words, the module thermal conductance nAk/L must be

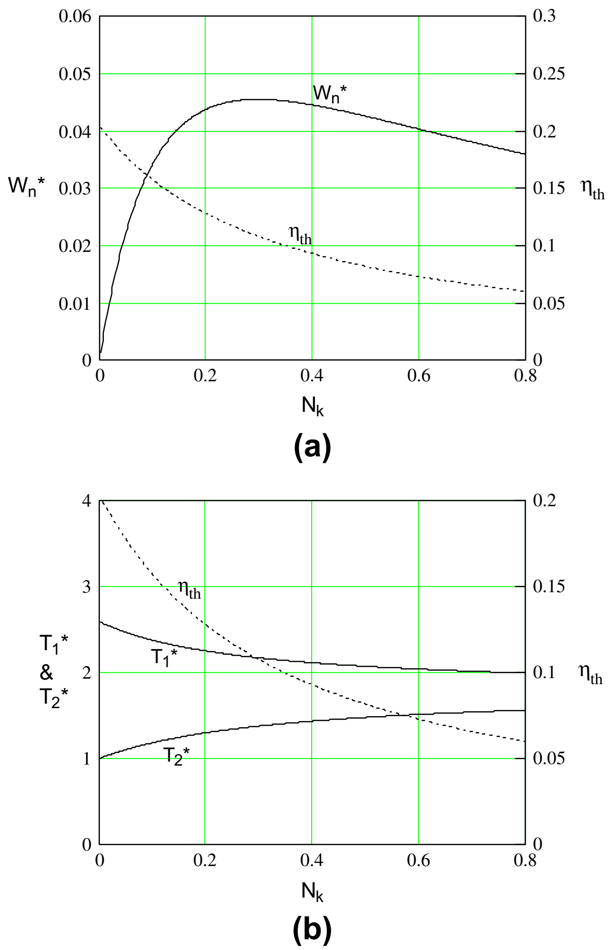

Fig. 3. (a) Dimensionless power output W_n^* and thermal efficiency η_{th} versus dimensionless thermal conductance N_k and (b) high and low junction temperatures (T_1^* and T_2^*) versus dimensionless thermal conductance N_k. These plots were generated using $N_h = 1$, $R_r = 1.7$, $T_\infty^* = 2.6$ and $ZT_{\infty 2} = 1.0$.

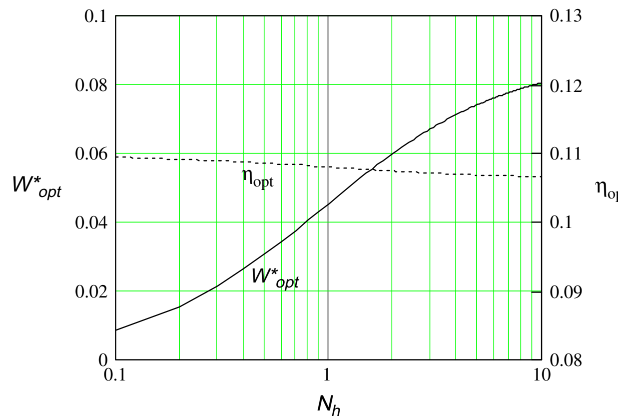

Fig. 4. Optimal dimensionless power output W_{opt}^* and efficiency η_{opt} versus dimensionless convection N_h. This plot was generated using $T_\infty^* = 2.6$ and $ZT_{\infty 2} = 1.0$.

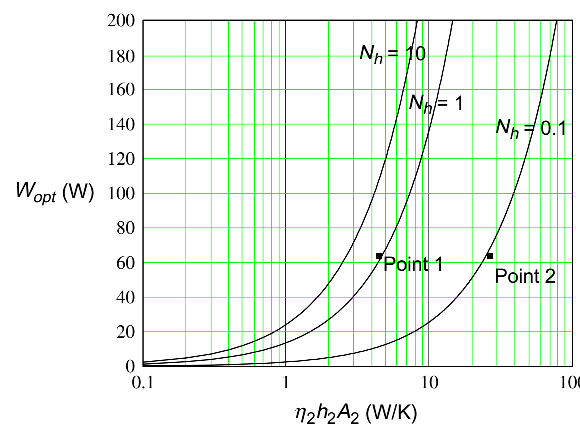

Fig. 5. Optimal power output W_{opt} versus convection conductance $\eta_2 h_2 A_2$ in fluid 2 as a function of dimensionless convection N_h. This plot was generated using $T_{\infty 2} = 25$ °C, $T_\infty^* = 2.6$ and $ZT_{\infty 2} = 1.0$.

redesigned on the basis of the $\eta_2 h_2 A_2$ to meet $N_k = 0.3$. The information of the optimal thermal conductance $[(n)(A/L)(k)]$ is particularly important in design of microstructured or thin-film thermoelectric devices. Furthermore, there is a potential to improve the performance or to provide the variety of the geometry by reducing the thermal conductivity k.

The dimensionless high and low junction temperatures are presented in Fig. 3b. As N_k decreases towards zero, T_1^* and T_2^* approach T_∞^* and 1, respectively. This indicates that the thermal resistances of two heat sinks approaches zero, which never happens. It is noted that the thermal efficiency approaches the theoretical maximum efficiency of 0.2 for the given fluid temperatures as N_k approaches zero.

Since there is an optimal combination of N_k and R_r for a given N_h, we can plot the optimal dimensionless power output W_{opt}^* and optimal thermal efficiency η_{opt} as a function of dimensionless convection N_h, which is shown in Fig. 4. It is very interesting to note in Fig. 4 that, with increasing N_h, η_{opt} barely changes, while W_{opt}^* monotonically increases. According to Eq. (14), the actual optimal power output W_{opt} is the product of W_{opt}^* and $\eta_2 h_2 A_2$, seemingly increasing linearly with $\eta_2 h_2 A_2$. In practice, there is a controversial tendency that N_h may decrease systematically with increasing $\eta_2 h_2 A_2$ if η_1 $h_1 A_1$ is limited. As a result of this, it is needed to examine the variety of the $\eta_2 h_2 A_2$ as a function of N_h for the optimal power output. Fig. 5 reveals the intricate relationship between $\eta_2 h_2 A_2$ and N_h (or $\eta_1 h_1 A_1$) along with the optimum actual power output (not dimensionless), which would lead system designers to a variety of possible allocations ($\eta_2 h_2$ A_2 and N_h) for their optimal design. Now we look into the actual optimal design with the actual values.

For example, using Figs. 4 and 5, we develop an optimal design for automobile exhaust gas waste heat recovery. A thermoelectric generator module with a 5-cm × 5-cm base area is subject to exhaust gases at 500 °C in fluid 1 and air at 25 °C in fluid 2. We estimate an available maximum convection conductance in fluid 1 (exhaust gas) with $\eta_1 = 0.8$, $h_1 = 60$ W/m^2 K, and $A_1 = 1000$ cm^2 and also an available maximum convection conductance in fluid 2 (air) with $\eta_2 = 0.8$, $h_2 = 60$ W/m^2 K, and $A_2 = 1000$ cm^2, which gives $\eta_1 h_1 A_1 = \eta_2 h_2 A_2 = 4.8$ W/K and $N_h = 1$. Note that η_1 and η_2 are typical fin efficiencies, and h_1 and h_2 are the reasonable convection coefficients for exhaust gas heating and air cooling, of which the convection coefficients with exhaust gas or air typically have values ranging between 20 and 100 W/m^2 K depending on the flow rate and the type of fin. The middle value of 60 W/m^2 K was used in the present work. Each area of A_1 and A_2 is based on 20 fins (two sides) with a fin height of 5 cm on a 5-cm × 5-cm base area of the module, which gives an total fin area (5 cm × 5 cm × 2 sides × 20 fins = 1000 cm^2). The typical thermoelectric material properties are assumed to be $\alpha_p = -\alpha_n = 220$ μV/K, $\rho_p = \rho_n = 1.0 \times 10^{-3}$ Ω cm, and $k_p = k_n = 1.4 \times 10^{-2}$ W/cm K. The above data approximately determines three dimensionless parameters as $N_h = 1$, $T_\infty^* = 2.6$ and $ZT_{\infty 2} = 1.0$.

Table 1
Inputs and results from the dimensional analysis for a TEG.

Inputs	Dimensionless $\left(W^*_{n,opt}\right)$	Actual ($W_{n,opt}$)
$T_{\infty 1}$ = 500 °C, $T_{\infty 2}$ = 25 °C, ΔT_∞ = 475 °C	N_k = 0.3	n = 254
A = 2 mm^2, L = 1 mm	N_h = 1	$\eta_1 h_1 A_1$ = 4.8 W/K
η_2 = 0.8, h_2 = 60 W/m^2 K, A_2 = 1000 cm^2	R_r = 1.7	R_L = 1.7 × n × R = 4.32 Ω
$\eta_2 h_2 A_2$ = 4.8 W/K	$T^*_\infty = 2.6$	$T_{\infty 1}$ = 500 °C
Base area A_b of module = 5 cm × 5 cm	$ZT_{\infty 2}$ = 1.0	$ZT_{\infty 2}$ = 1.0
$\alpha_p = -\alpha_n$ = 220 μV/K	$T^*_1 = 2.172$	T_1 = 374 °C
$\rho_p = \rho_n$ = 1.0 × 10^{-3} Ω cm	$T^*_2 = 1.367$	T_2 = 137 °C
$k_p = k_n$ = 1.4 × 10^{-2} W/cm K	$W^*_n = 0.045$	W_n = 65.0 W
(Z = 3.457 × 10^{-3} K^{-1})	η_{th} = 0.108	η_{th} = 0.108
(R = 0.01 Ω per thermocouple)	N_I = 0.306	I = 3.9 A
(η_1 = 0.8, h_1 = 60 W/m^2 K, A_1 = 1000 cm^2)	N_V = 0.50	V = 16.7 V
(Power density $P_d = W_n/A_b$)	–	P_d = 2.6 W/cm^2

As mentioned before, the present dimensional analysis enables the three dimensionless parameters (N_h = 1, $T^*_\infty = 2.6$ and $ZT_{\infty 2}$ = 1.0) to determine the rest two optimal parameters, which are found to be N_k = 0.3 and R_r = 1.7 as shown before. This leads to a statement that, if two individual fluid temperatures on heat sinks connected to a thermoelectric generator module are given, an optimum design always exists with the feasible mechanical constraints that present N_h. This optimal design is indicated approximately at Point 1 in Fig. 5. Note that there are ways to improve the optimal power output, increasing either $\eta_2 h_2 A_2$ or N_h or both, which obviously depends on the feasible mechanical constraints, whichever is available.

The inputs and optimum results at Point 1 in Fig. 5 are summarized in Table 1. The inputs are the geometry of thermocouple, the material properties, two fluid temperatures, and the available convection conductance in fluid 2. The dimensionless results are converted to the actual quantities as shown. The maximum power output is found to be 65.0 W for the 5 cm × 5 cm base area of the module. The power density is calculated to be 2.6 W/cm^2, which appears significantly high compared to an available power density of ∼1 W/cm^2 with the similar operating conditions by NEDO program (Japan) [7].

Air was used in fluid 2 so far. However, we want to see the effect of $\eta_2 h_2 A_2$ or N_h by changing fluid 2 from air to liquid coolant. Otherwise the same conditions were applied to as the previous example. We then estimate an available convection conductance in fluid 1 (exhaust gas) with the same one of η_1 = 0.8, h_1 = 60 W/m^2 K, and A_1 = 1000 cm^2, but an available convection conductance in fluid 2 (liquid coolant) with η_2 = 0.8, h_2 = 3000 W/m^2 K, and A_2 = 100 cm^2, which gives $\eta_1 h_1 A_1$ = 4.8 W/K and $\eta_2 h_2 A_2$ = 24 W/K, respectively, which yields N_h = 0.1. The area of A_1 is based on 20 fins (two sides) with a fin height of 5 cm for the 5-cm × 5-cm base area of the module and A_2 is estimated to be one tenth of A_1 (liquid coolant does not require a large heat transfer area). These inputs and optimum results give all the five dimensionless parameters as $N_k = 0.07$, $N_h = 0.1$, $R_r = 1.5$, $T^*_\infty = 2.6$ and $ZT_{\infty 2}$ = 1.0, for which the optimum at $\eta_2 h_2 A_2$ = 24 W/K is indicated at Point 2 in Fig. 5. The effect of N_h on the high and cold junction temperatures was also presented in Fig. 6. It is interesting to see that, although a small variation in the optimal power outputs between Point 1 (N_h = 1) and Point 2 (N_h = 0.1) appears in Fig. 5, a significant temperature variation between N_h = 1 and N_h = 0.1 appears in Fig. 6. This may be an important factor particularly when thermoelectric materials are considered in the optimal design. The proximity of the power outputs between Points 1 and 2 is an example showing the variety of the mechanical constraints ($\eta_1 h_1 A_1$ and $\eta_2 h_2 A_2$) even with the same power outputs. It is important to realize that, when $\eta_1 h_1 A_1$ is limited, simply increasing $\eta_2 h_2 A_2$ invokes decreasing N_h, which results in decreasing not only the high and cold junction temperatures but also slightly the temperature difference as shown in Fig. 6. The coexistence that the Seebeck coefficient decreases with decreasing the temperature and reducing the temperature difference diminishes the performance will cause the power output to decline. However, increasing $\eta_2 h_2 A_2$ will directly increase the power output as mentioned earlier. The net power output of loss and gain by increasing $\eta_2 h_2 A_2$ may be a role of system designer. Anyhow there will be a small change in the efficiency.

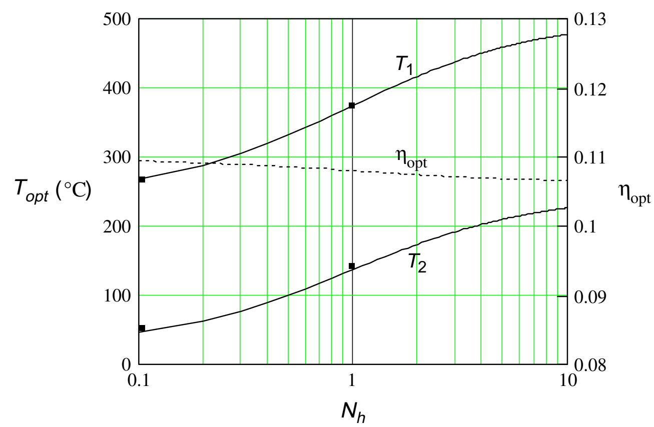

Fig. 6. Hot and cold junction temperatures and optimal efficiency versus dimensionless convection. This plot was generated with $T_{\infty 2}$ = 25 °C, $T^*_\infty = 2.6$ and $ZT_{\infty 2}$ = 1.0.

2. Thermoelectric cooler

Let us consider a simplified steady-state heat transfer on a thermoelectric cooler module (TEC) with two heat sinks as shown in Fig. 7. Each heat sink faces a fluid flow at temperature T_∞. Subscripts 1 and 2 denote the entities of fluids 1 and 2, respectively. Consider that an electric current is directed in a way that the cooling power Q_1 enters heat sink 1. We assume that the electrical and thermal contact resistances in the TEC are negligible, the material properties are independent of temperature, and also the TEC is perfectly insulated. The TEC has a number of thermocouples, of which each thermocouple consists of p-type and n-type thermoelements with the same dimensions.

The basic equations for the TEC with two heat sinks are given by

$$Q_1 = \eta_1 h_1 A_1 (T_{\infty 1} - T_1) \tag{25}$$

$$Q_1 = n\left(\alpha I T_1 - \frac{1}{2} I^2 R + \frac{Ak}{L}(T_1 - T_2)\right) \tag{26}$$

$$Q_2 = n\left(\alpha I T_2 + \frac{1}{2} I^2 R + \frac{Ak}{L}(T_1 - T_2)\right) \tag{27}$$

$$Q_2 = \eta_2 h_2 A_2 (T_2 - T_{\infty 2}) \tag{28}$$

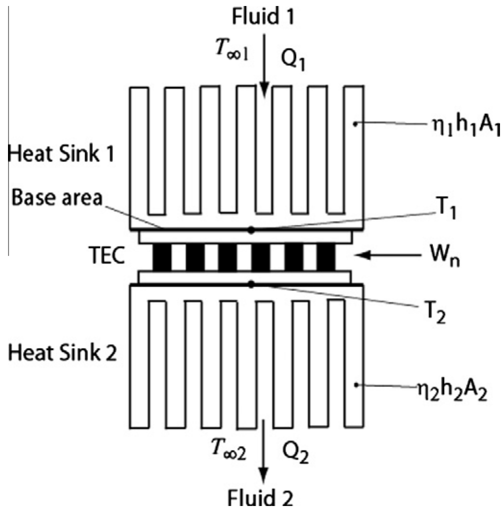

Fig. 7. Thermoelectric cooler module (TEC).

where $\alpha = \alpha_p - \alpha_n$, $k = k_p + k_n$, and $\rho = \rho_p + \rho_n$. In order to study the optimization of the TEC, several dimensionless parameters are introduced. The dimensionless thermal conductance, which is the ratio of thermal conductance to the convection conductance in fluid 2, is

$$N_k = \frac{n(Ak/L)}{\eta_2 h_2 A_2} \tag{29}$$

The dimensionless convection, which is the ratio of convection conductance in fluid 1 to fluid 2, is

$$N_h = \frac{\eta_1 h_1 A_1}{\eta_2 h_2 A_2} \tag{30}$$

The dimensionless current is given by

$$N_I = \frac{\alpha I}{Ak/L} \tag{31}$$

The dimensionless temperatures are defined by

$$T_1^* = \frac{T_1}{T_{\infty 2}} \tag{32}$$

$$T_2^* = \frac{T_2}{T_{\infty 2}} \tag{33}$$

$$T_\infty^* = \frac{T_{\infty 1}}{T_{\infty 2}} \tag{34}$$

The dimensionless cooling power, rate of heat liberated and electrical power input are defined by

$$Q_1^* = \frac{Q_1}{\eta_2 h_2 A_2 T_{\infty 2}} \tag{35}$$

$$Q_2^* = \frac{Q_2}{\eta_2 h_2 A_2 T_{\infty 2}} \tag{36}$$

$$W_n^* = \frac{W_n}{\eta_2 h_2 A_2 T_{\infty 2}} \tag{37}$$

It is noted that the above dimensionless parameters are based on the convection conductance in fluid 2, which means that $\eta_2 h_2 A_2 T_{\infty 2}$ should be initially provided. Using the dimensionless parameters defined in Eqs. (29)–(34), Eqs. (25)–(28) reduce to two formulas as:

$$\frac{N_h(T_\infty^* - T_1^*)}{N_k} = N_I T_1^* - \frac{N_I^2}{2ZT_{\infty 2}} + (T_1^* - T_2^*) \tag{38}$$

$$\frac{T_2^* - 1}{N_k} = N_I T_2^* + \frac{N_I^2}{2ZT_{\infty 2}} + (T_1^* - T_2^*) \tag{39}$$

Eqs. (38) and (39) can be solved for T_1^* and T_2^*. The dimensionless temperatures are then a function of five independent dimensionless parameters as

$$T_1^* = f(N_k, N_h, N_I, T_\infty^*, ZT_{\infty 2}) \tag{40}$$

$$T_2^* = f(N_k, N_h, N_I, T_\infty^*, ZT_{\infty 2}) \tag{41}$$

T_∞^* is the input and $ZT_{\infty 2}$ is the material property with the input, and both are initially provided. Therefore, the optimization can be performed only with the first three parameters (N_k, N_h, and N_I). Once the two dimensionless temperatures (T_1^* and T_2^*) are solved for, the dimensionless rates of heat transfer at both junctions of the TEC can be obtained as:

$$Q_1^* = N_h(T_\infty^* - T_1^*) \tag{42}$$

$$Q_2^* = T_2^* - 1 \tag{43}$$

Q_1^* is called the dimensionless cooling power. Then, we have the dimensionless power input as

$$W_n^* = Q_2^* - Q_1^* \tag{44}$$

Accordingly, the coefficient of performance is obtained by

$$COP = \frac{Q_1^*}{W_n^*} \tag{45}$$

Defining $N_V = V/n\alpha T_{\infty 2}$, the dimensionless voltage is obtained by

$$N_V = \frac{W_n^*}{N_I N_k} \tag{46}$$

With the inputs (T_∞^* and $ZT_{\infty 2}$), we try to find the optimal combination for the dimensionless parameters (N_k,N_h, and N_I) iteratively until they converge. It is found that both N_k and N_I show the optimal values for the dimensionless cooling power Q_1^*, while N_h does not show the optimal value showing that the dimensionless cooling power Q_1^* monotonically increases with increasing N_h. This implies that, if any N_h is given, the optimal combination of N_k and N_I can be obtained. However, the dimensionless convection N_h actually presents the feasible mechanical constraints. Thus, we proceed with a typical value of $N_h = 1$ for illustration and later examine the variety of N_h with a practical design example.

Suppose that we have $T_\infty^* = 0.967$ (two arbitrary fluid temperatures) and $ZT_{\infty 2} = 1.0$ (materials) along with $N_h = 1$ as inputs. Then, we can determine the optimal combination for N_I and N_k, which may be obtained either graphically or using a computer program. We first use the graphical method at this moment and later the program for multiple computations (a Mathematical software Mathcad was used). The optimal combination of N_I and N_k for each

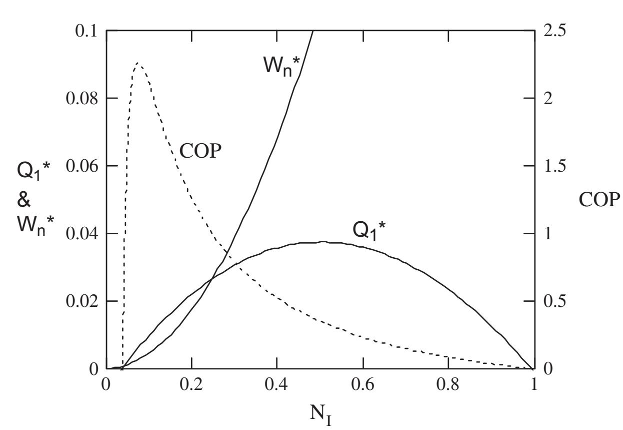

Fig. 8. Dimensionless cooling power Q_1^*, power input W_n^* and COP versus dimensionless current N_I. This plot was generated with $N_k = 0.3$, $N_h = 1$, $T_\infty^* = 0.967$ and $ZT_{\infty 2} = 1.0$.

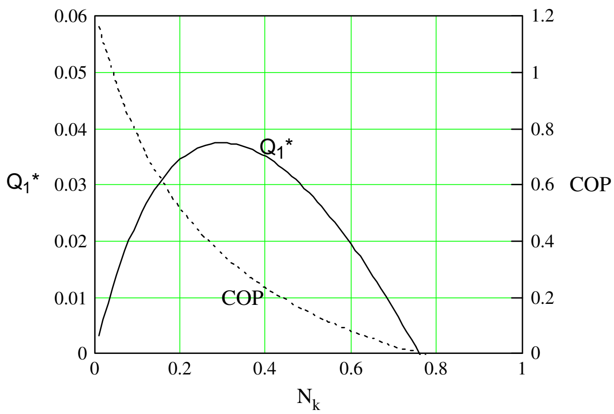

Fig. 9. Dimensionless cooling power Q_1^* and COP versus dimensionless thermal conductance N_k. This plot was generated with $N_h = 1$, $N_I = 0.5$, $T_\infty^* = 0.967$ and $ZT_{\infty 2} = 1.0$.

maximum cooling power are found to be $N_I = 0.5$ and $N_k = 0.3$, respectively, which are shown in Figs. 8 and 9. The maximum cooling power of $Q_1^* = 0.037$ in both figures is actually the optimal dimensionless cooling power $Q_{1,opt}^*$. However, the *COP* also shows an optimal value at $N_I = 0.074$, which gives $Q_1^* = 0.006$. The optimal *COP* usually gives a very small cooling power or sometimes even no exists, which seems impractical, albeit the high *COP*. Therefore, it is needed to have a practical point for the optimal *COP*, which is determined in the present work to be the midpoints of the optimumN_I and N_k. For example, the practical optimal *COP* in this case occurs simultaneously at $N_I = 0.25$ and $N_k = 0.15$, which leads to $Q_1^* = 0.019$ that may be seen after re-plotting with the two values.

The existence of an optimum cooling power as a function of current is a well known characteristic of TECs. However, the existence of the optimum N_k in TECs has not been found in the literature to the author's knowledge. With Eq. (29) that is $N_k = n(Ak/L)/\eta_2 h_2 A_2$, the optimum of $N_k = 0.3$ implies that the module thermal conductance $n(Ak/L)$ is at optimum since the $\eta_2 h_2 A_2$ is given, which leads to the optimum n (the number of thermocouples) if Ak/L is given or vice versa. This is one of the most important optimum processes in design of a thermoelectric cooler module. It is good to know in Fig. 10 that the dimensionless temperature T_1^* becomes lowest at the optimal dimensionless cooling power Q_1^*, not at the optimum *COP*.

We also consider two heat sinks as a unit without a TEC to examine the limitation of use of the TEC, which is shown in Fig. 11. The geometry of the unit is the same as the one shown in Fig. 7 except that there is no TEC between the heat sinks. There should be a cooling rate with given fluid temperatures, which is

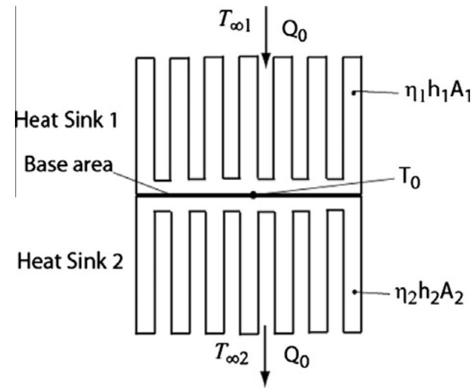

Fig. 11. Heat sinks without a TEC.

Q_0. We want to compare the cooling power Q_1 with this cooling rate Q_0 to determine the limit of use of the TEC.

The basic equations for the unit can be expressed as

$$Q_0 = \eta_1 h_1 A_1 (T_{\infty 1} - T_0) \tag{47}$$

$$Q_0 = \eta_2 h_2 A_2 (T_0 - T_{\infty 2}) \tag{48}$$

The dimensionless groups for the unit are

$$T_0^* = \frac{T_0}{T_{\infty 2}} \tag{49}$$

$$Q_0^* = \frac{Q_0}{\eta_2 h_2 A_2 T_{\infty 2}} \tag{50}$$

Using Eqs. (30), (34), (49) and (50), Eqs. (47) and (48) reduce to a formula as

$$T_0^* = \frac{N_h T_\infty^* + 1}{N_h + 1} \tag{51}$$

The dimensionless cooling rate without heat sinks can be obtained by

$$Q_0^* = T_0^* - 1 \tag{52}$$

The dimensionless cooling power Q_1^* and cooling rate of the unit Q_0^* versus the dimensionless fluid temperature T_∞^* along with the *COP* are presented in Fig. 12. The cross point in the figure is found to be $T_\infty^* = 1.2$, which is a design point as the limit of use of the TEC. If the dimensionless fluid temperature T_∞^* is higher than the cross point, there is no justification for use of the TEC although the TEC still functions. This cross point is defined as the maximum dimensionless temperature $T_{\infty,\max}^*$. There is also a minimum point

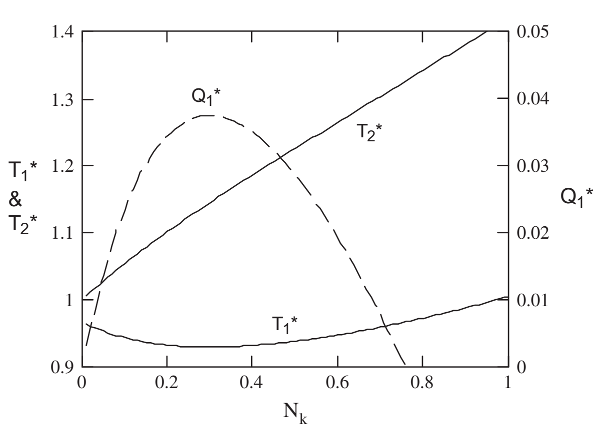

Fig. 10. Dimensionless temperatures versus dimensionless thermal conductance. This plot was generated with $N_h = 1$, $N_I = 0.5$, $T_\infty^* = 0.967$ and $ZT_{\infty 2} = 1.0$.

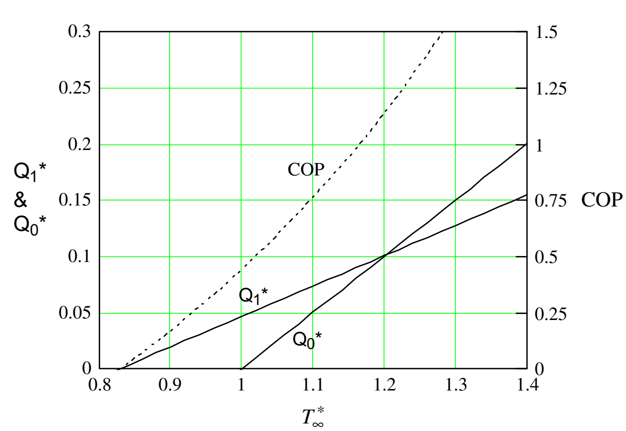

Fig. 12. Dimensionless cooling power, cooling rate of the unit, and COP versus dimensionless fluid temperature. This plot was generated with $N_k = 0.3$, $N_h = 1$, $N_I = 0.5$ and $ZT_{\infty 2} = 1.0$.

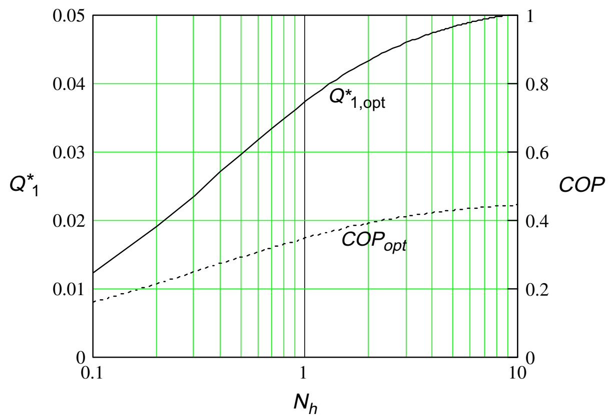

Fig. 13. Optimal (cooling power optimized) dimensionless cooling power and *COP* versus dimensionless convection. This plot was generated with $T^*_\infty = 0.967$ and $ZT_{\infty 2} = 1.0$.

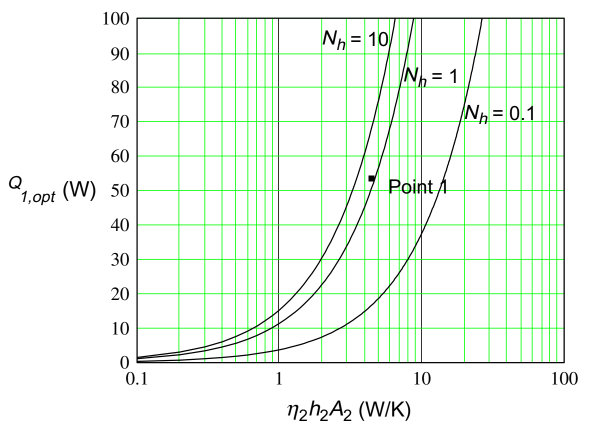

Fig. 14. Optimal cooling power versus convection conductance in fluid 2 as a function of dimensionless convection. This plot was generated with $T_{\infty 2}$ = 30 °C, $T^*_\infty = 0.967$ and $ZT_{\infty 2} = 1.0$.

at $T^*_\infty = 0.83$, where $Q^*_1 = 0$, which is called the minimum dimensionless temperature $T^*_{\infty,\min}$. Note that the TEC can perform effective cooling within a range from $T^*_{\infty,\min} = 0.83$ to $T^*_{\infty,\max} = 1.2$.

Since there is an optimal combination of N_I and N_k for a given N_h, we can plot the optimal dimensionless cooling power $Q^*_{1,opt}$ and COP_{opt} as a function of dimensionless convection N_h, which is shown in Fig. 13. It is seen that both $Q^*_{1,opt}$ and COP_{opt} increase monotonically with increasing N_h. According to Eq. (35), the actual optimal cooling power $Q_{1,opt}$ is the product of $Q^*_{1,opt}$ and $\eta_2 h_2 A_2$, seemingly increasing linearly with $\eta_2 h_2 A_2$. In practice, there is a controversial tendency that N_h may decrease systematically with increasing $\eta_2 h_2 A_2$. As a result of this, it is needed to examine the variety of the $\eta_2 h_2 A_2$ as a function of N_h for the optimal cooling power. Fig. 14 reveals the intricate relationship between $\eta_2 h_2 A_2$ and N_h (or $\eta_1 h_1 A_1$) along with the optimum actual cooling power (not dimensionless), which would lead system designers to a variety of possible allocations ($\eta_2 h_2 A_2$ and N_h) for their optimal design. Note that the analysis so far is entirely based on the dimensionless parameters. Now we look into the actual optimal design with the actual values.

For example, using Figs. 13 and 14, we develop an optimal design for an automobile air conditioner. A thermoelectric cooler module with a 5-cm × 5-cm base area is subject to cabin air at 20 °C in fluid 1 and ambient air at 30 °C in fluid 2. We estimate an available maximum convection conductance in fluid 1 (cabin air) with η_1 = 0.8, h_1 = 60 W/m^2 K, and A_1 = 1000 cm^2 and also an available maximum convection conductance in fluid 2 (ambient air) with η_2 = 0.8, h_2 = 60 W/m^2 K, and A_2 = 1000 cm^2, which gives $\eta_1 h_1 A_1 = \eta_2 h_2 A_2$ = 4.8 W/K and N_h = 1. Note that η_1 and η_2 are the fin efficiencies, and h_1 and h_2 are the reasonable convection coefficients for the cabin air cooling and the ambient air cooling, respectively. Each area of A_1 and A_2 is based on 20 fins (two sides) with a fin height of 5 cm on a 5-cm × 5-cm base area of the module. The typical thermoelectric material properties are assumed to be $\alpha_p = -\alpha_n$ = 220 μV/K, $\rho_p = \rho_n = 1.0 \times 10^{-3}$ Ω cm, and $k_p = k_n = 1.4 \times 10^{-2}$ W/cm K. The above data approximately determines three dimensionless parameters as $N_h = 1$, $T^*_\infty = 0.967$ and $ZT_{\infty 2}$ = 1.0.

As mentioned before, the present dimensional analysis enables the three dimensionless parameters (N_h = 1, $T^*_\infty = 0.967$ and $ZT_{\infty 2}$ = 1.0) to determine the rest optimal parameters, which are found to be N_k = 0.3 and N_I = 0.5 as shown before. This leads to a statement that, if two individual fluid temperatures on heat sinks connected to a thermoelectric cooler module are given, an optimum design always exists with the feasible mechanical constraints that present N_h. This optimal design is indicated approximately at Point 1 in Fig. 14. Note that there are several ways to improve the optimal power output by increasing either $\eta_2 h_2 A_2$ or N_h or both, which apparently depends on the feasible mechanical constraints, whichever is available.

The inputs and optimum results at Point 1 in Fig. 14 are summarized in the first two columns of Table 2. The inputs are the geometry of thermocouple, the material properties, two fluid temperatures, and the available convection conductance in fluid 2. The dimensionless results are converted to the actual quantities. The optimal cooling power is found to be 54.4 W for the 5 cm × 5 cm base area of the module. The cooling power density is calculated to be 2.18 W/cm^2. When $\eta_1 h_1 A_1$ is limited, simply increasing $\eta_2 h_2 A_2$ invokes decreasing N_h, which is shown in Fig. 15. This attributes to the heat balance that the hot and cold junction temperatures must decrease when more heat is extracted

Table 2
Inputs and results from the dimensional analysis for a thermoelectric cooler module.

Input	$Q^*_{1,opt}$ (dimensionless)	$Q_{1,opt}$ (actual)	$COP_{1/2opt}$ (dimensionless)	$COP_{1/2opt}$ (actual)
$T_{\infty 1}$ = 20 °C, $T_{\infty 2}$ = 30 °C	N_k = 0.3	n = 257	N_k = 0.15	n = 128
A = 2 mm^2, L = 1 mm	N_h = 1	$\eta_1 h_1 A_1$ = 4.8 W/K	N_h = 1	$\eta_1 h_1 A_1$ = 4.8 W/K
η_2 = 0.8, h_2 = 60 W/m^2 K,	N_I = 0.5	I = 6.36 A	N_I = 0.25	I = 3.18 A
A_2 = 1000 cm^2	$T^*_\infty = 0.967$	$T_{\infty 1}$ = 20 °C	$T^*_\infty = 0.967$	$T_{\infty 1}$ = 20 °C
Base area A_b = 5 cm × 5 cm	$ZT_{\infty 2}$ = 1.0	$ZT_{\infty 2}$ = 1.0	$ZT_{\infty 2}$ = 1.0	$ZT_{\infty 2}$ = 1.0
$\alpha_p = -\alpha_n$ = 220 μV/K	$T^*_1 = 0.930$	T_1 = 8.7 °C	$T^*_1 = 0.949$	T_1 = 14.4 °C
$\rho_p = \rho_n = 1.0 \times 10^{-3}$ Ω cm	$T^*_2 = 1.145$	T_2 = 73.9 °C	$T^*_2 = 1.031$	T_2 = 39.4 °C
$k_p = k_n = 1.4 \times 10^{-2}$ W/cm K	$Q^*_1 = 0.037$	Q_1 = 54.4 W	$Q^*_1 = 0.019$	Q_1 = 26.9 W
($Z = 3.457 \times 10^{-3}$ K^{-1})	COP = 0.35	COP = 0.35	COP = 1.49	COP = 1.49
(R = 0.01 Ω per thermocouple)	N_V = 0.715	V_n = 24.5 V	N_V = 0.332	V_n = 5.7 V
	$T^*_{\infty,\max} = 1.2$	$T_{\infty 1,max}$ = 91.3 °C	$T^*_{\infty,\max} = 1.06$	$T_{\infty 1,max}$ = 49.7 °C
	$T^*_{\infty,\min} = 0.83$	$T_{\infty 1,min}$ = −21.8 °C	$T^*_{\infty,\min} = 0.84$	$T_{\infty 1,min}$ = −19.2 °C
(Cooling power density $P_d = Q_1/A_b$)	–	P_d = 2.18 W/cm^2	–	P_d = 1.08 W/cm^2

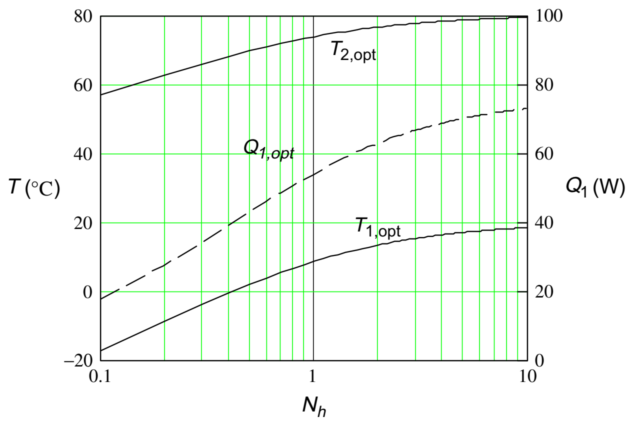

Fig. 15. Two junction temperatures and cooling power versus convection conductance in fluid 2. This plot was generated with, $\eta_2 h_2 A_2 = 4.8$ W/K $T_{\infty 2} = 30$ °C, $T^*_\infty = 0.967$ and $ZT_{\infty 2} = 1.0$.

from the limited input, which is a characteristic of the thermoelectric cooler with heat sinks. The hot and cold junction temperatures are sometimes a design factor, noting that the optimal cold junction temperature $T_{1,opt}$ reaches zero Celsius at $N_h = 0.4$, which may cause icing and reducing the heat transfer.

As mentioned before, the optimal *COP* is sometimes in demand in addition to the optimal cooling power. However, the real optimal *COP* usually gives a very small value of the cooling power, albeit the high *COP*. Therefore, in the present work, the midpoints of the optimal N_I and N_k are used to provide approximately a half of the optimal cooling power and at least four folds of the cooling-power-optimized *COP*. This modified optimal *COP* is called a half optimal coefficient of performance $COP_{1/2opt}$. These results are also tabulated in the last two columns of Table 2, so that designers could determine which optimum is better depending on the application. The optimum cooling power is usually selected when the resources (electrical power or capacity of coolant) are abundant or inexpensive or the efficacy is not important as in microprocessor cooling, while the half optimum *COP* is selected when the resources are limited or expensive or the efficacy is important as in automotive air conditioners.

3. Conclusions

The present paper presents the optimal design of thermoelectric devices in conjunction with heat sinks introducing new dimensionless parameters. The present optimum design includes the power output (or cooling power) and the efficiency (or COP) simultaneously with respect to the external load resistance (or electrical current) and the geometry of thermoelements. The optimal design provides optimal dimensionless parameters such as the thermal conduction ratio, the convection conduction ratio, and the load resistance ratio as well as the cooling power, efficiency and high and low junction temperatures. The load resistance ratio (or the electrical current) is a well known characteristic of optimum design. However, it is found that the load resistance ratio would be greater than unity (1.7 in the present case). This is a confusing factor in optimum design with a TEG. One should not assume that the load resistance ratio R_L/R is equal to unity for a TEG with heat sink(s). The optimal thermal conductance $[(n)(A/L)(k)]$ consists of the number of thermocouples, the geometric ratio, and the thermal conductivity. It is important that there is an optimum number of thermocouples n for a given the convection conductance $\eta_2 h_2 A_2$ if the optimal thermal conductance A/L is constant or vice versa. These are the optimum geometry of thermoelectric devices. The information of the optimal thermal conductance is particularly important in design of microstructured or thin-film thermoelectric devices. Furthermore, there is a potential to improve the performance or to provide the variety of the geometry by reducing the thermal conductivity.

Finally, it is stated from the present dimensional analysis that, if two individual fluid temperatures on heat sinks connected to a thermoelectric generator or cooler are given, an optimum design always exists and can be found with the feasible mechanical constraints.

References

[1] Kraemer D, McEnaney K, Chiesa M, Chen G. Modeling and optimization of solar thermoelectric generators for terrestrial applications. Solar Energy 2012;86:1338–50.
[2] Karri MA, Thacher EF, Helenbrook BT. Exhaust energy conversion by thermoelectric generator: two case studies. Energy Convers Manage 2011;52:1596–611.
[3] Hsu CT, Huang GY, Chu HS, Yu B, Yao DJ. Experiments and simulations on low-temperature waste heat harvesting system by thermoelectric power generators. Appl Energy 2011;88:1291–7.
[4] Henderson J. Analysis of a heat exchanger–thermoelectric generator system. In: 14th Intersociety energy conversion engineering conference, Boston, Massachusetts; August 5–10, 1979.
[5] Stevens JW. Optimal design of small ΔT thermoelectric generation systems. Energy Convers Manage 2001;42:709–20.
[6] Crane DT, Jackson GS. Optimization of cross flow heat exchangers for thermoelectric waste heat recovery. Energy Convers Manage 2004;45:1565–82.
[7] Rowe DM. Thermoelectrics handbook: micro to nano. New York: Taylor & Francis; 2006.
[8] Chein R, Huang G. Thermoelectric cooler application in electronic cooling. Appl Therm Eng 2004;24:2207–17.
[9] Vining CB. An inconvenient truth about thermoelectrics. Nat Mater 2009;8.
[10] Wang CC, Hung CI, Chen WH. Design of heat sink for improving the performance of thermoelectric generator using two-stage optimization. Energy 2012;39:236–45.
[11] Zhang HY. A general approach in evaluating and optimizing thermoelectric coolers. Int J Refrig 2010;33:1187–96.
[12] Luo J, Chen L, Sun F, Wu C. Optimum allocation of heat transfer surface area for cooling load and COP optimization of a thermoelectric refrigerator. Energy Convers Manage 2003;44:3197–206.
[13] Chen L, Li J, Sun F, Wu C. Performance optimization of a two-stage semiconductor thermoelectric–generator. Appl Energy 2005;82:300–12.
[14] Yazawa K, Shakouri A. Optimization of power and efficiency of thermoelectric devices with asymmetric thermal contacts. J Appl Phys 2012;111:024509.
[15] Chen L, Gong J, Sun F, Wu C. Effect of heat transfer on the performance of thermoelectric generators. Int J Therm Sci 2002;41:95–9.
[16] Mayer PM, Ram RJ. Optimization of heat sink-limited thermoelectric generators. Nanoscale Microscale Thermophys Eng 2006;10:143–55.
[17] Yilbas BS, Sahin AZ. Thermoelectric device and optimum external load parameter and slenderness ratio. Energy 2010;35:5380–4.
[18] Chen L, Meng F, Sun F. Effect of heat transfer on the performance of thermoelectric generator-driven thermoelectric refrigerator system. Cryogenics 2012;52:58–65.
[19] Chen L, Li J, Sun F, Wu C. Performance optimization for a two-stage thermoelectric heat-pump with internal and external irreversibilities. Appl Energy 2008;85:641–9.
[20] Xuan XC. On the optimal design of multistage thermoelectric coolers. Semicond Sci Technol 2002;17:625–9.
[21] Yamanashi M. A new approach to optimum design in thermoelectric cooling systems. J Appl Phys 1996;80(9):5494–502.
[22] Xuan XC. Optimum design of a thermoelectric device. Semicond Sci Technol 2002;17:114–9.
[23] Nagy MJ, Buist R. Effect of heat sink design on thermoelectric cooling performance. Am Inst Phys 1995:147–9.
[24] Pan Y, Lin B, Chen J. Performance analysis and parametric optimal design of an irreversible multi-couple thermoelectric refrigerator under various operating conditions. Appl Energy 2007;84:882–92.
[25] Casano G, Piva S. Parametric thermal analysis of the performance of a thermoelectric generator. In: 6th European thermal sciences conference (Eurotherm 2012), Journal of Physics: Conference Series, 395, 012156; 2012.
[26] Goktun S. Design considerations for a thermoelectric refrigerator. Energy Convers Manage 1995;36(12):1197–200.
[27] Gou X, Xiao H, Yang S. Modeling, experimental study and optimization on low-temperature waste heat thermoelectric generator system. Appl Energy 2010;87:3131–6.
[28] Chang Y, Chang C, Ke M, Chen S. Thermoelectric air-cooling module for electronic devices. Appl Therm Eng 2009;29:2731–7.
[29] Huang H, Weng Y, Chang Y, Chen S, Ke M. Thermoelectric water-cooling device applied to electronic equipment. Int Commun Heat Mass Transfer 2010;37:140–6.
[30] Casano G, Piva S. Experimental investigation of the performance of a thermoelectric generator based on Peltier cells. Exp Therm Fluid Sci 2011;35:660–9.